A Smart Antenna Array for Brain Cancer Detection

Haoyu Zhang, Ahmed O. El-Rayis, Nakul Haridas, Nurul H. Noordin, Ahmet T. Erdogan, Tughrul Arslan

Advanced Smart Antenna Technologies Research Group, School of Engineering, The University of Edinburgh, EH9 3JL, UK

{H.Zhang, A.El-Rayis, N.Haridas, N.Noordin, Ahmet.Erdogan, T.Arslan}@ed.ac.uk

***Abstract*— A smart antenna array is designed and fabricated for brain cancer detection. The smart antenna array is composed of three ultra-wideband vivaldi antennas. A brain model with 4 layers is created and simulated with the CST Microwave Studio. A radius of 5mm tumour model is placed into the white matter close to the skull. A short pulse is transmitted into the brain and the reflected signals are detected by one or more receiver antennas placed in different positions. Analysis of the reflected signals shows that using a smart antenna array based imaging system can be used for brain cancer detection.**

I. INTRODUCTION

Microwave imaging based cancer detection has become an interesting research area in recent years. The working principle is based on the high dielectric difference between the tumour and healthy tissue [1]. The tumour can be detected from the back-scattered signals. There are many approaches based on the microwave image cancer detection. One approach is called microwave tomography [2]. It is similar to MRI, which aims at creating the cross-section image of the body by scattered energy. The advantages of the microwave tomography include the whole view of body tissue; however, the problem is that every tissue is not clearly identifiable [3]. Furthermore, the signal processing is very complex which requires solving non-linear functions. Another alternative approach is the use of ultra-wideband (UWB) antennas [4], in which a short pulse is transmitted into the body [5] [6]. Then the reflected signals are detected by one or more receiver antennas placed in different locations. Moreover, by using phase or time shift, more sets of signals can be collected for calibration in order to reduce noise and clutter.

In this paper, we present a smart antenna array for brain cancer detection. The antenna array is composed of three ultra-wideband vivaldi antennas which have relatively small dimensions and provide good performance. This paper is organized as follows: Section II introduces the vivaldi antenna structure, simulated and measured performance. Simulation results obtained with breast and brain models generated by the CST Microwave Studio are presented in Section III. Finally, discussion and conclusions are provided in Section IV.

II. THE ANTENNA STRUCTURE AND PERFORMANCE

The geometry of the designed vivaldi antenna is shown in Fig. 1 (a). This is an antenna with a microstrip to slot line transition. The microstrip line incorporates a tapered section to match the input impedance to 50Ω. For the fabrication, a FR4 (ε_r=4.3) substrate is used whose thickness is 1.6mm and has 35μm copper on both sides. The length (L) and width (W) of the fabricated antenna array are 73.4mm and 41.9mm, respectively. Fig. 1 (b) is the photo of the fabricated antenna.

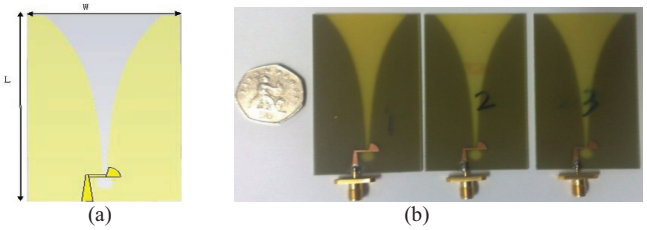

(a) (b)

Fig. 1 (a) Schematic of the designed vivaldi antenna, (b) the fabricated vivaldi antenna.

The simulated reflection coefficient of the vivaldi antenna is shown in Fig. 2 (a). As can be seen, the return loss is more than 10 db from 5 GHz to 10 GHz, except around 5.9 GHz. Practical measurement results (Fig. 2 (b)) demonstrate a good match with the simulation results from 5 GHz to 10 GHz.

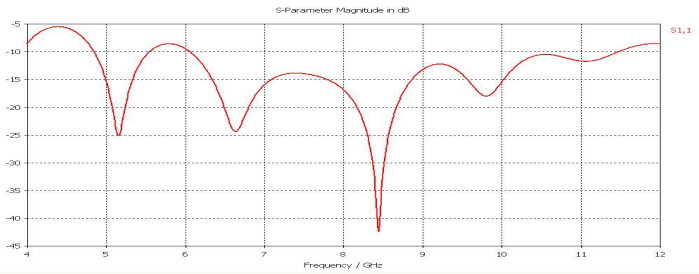

(a)

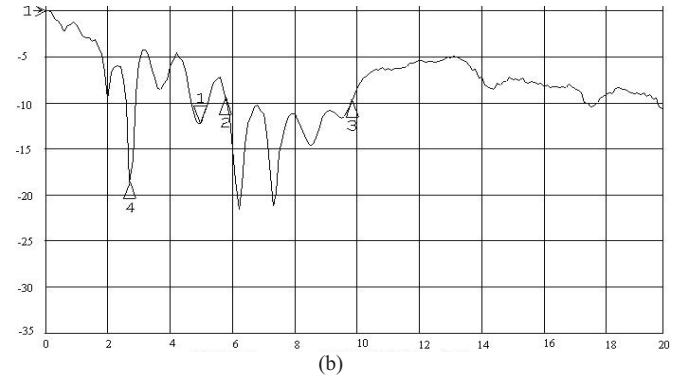

(b)

Fig. 2 (a) Simulated S11 and (b) measured S11 characteristics of the vivaldi antenna.

Fig. 3 (a) and (b) illustrate the E-field and radiation pattern, respectively. This shows that the designed vivaldi antenna has a very good directivity. The pencil beam ensures that sufficient energy penetrates the body object. Furthermore, the very slim beam allows targeting very small tumours or other objects when scanning the body.

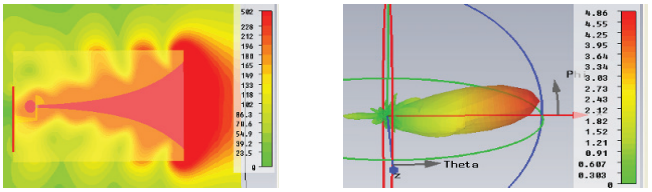

(a) (b)

Fig. 3. Simulation results for (a) E-Field and (b) the radiation pattern.

III. EXPERIMENTS

Two experiments were performed as follows: 1) A tumour model is placed in different locations within the brain model and the reflected signals from the tumour are recorded and compared. 2) Three antennas are aligned in parallel with 15mm distance between them. A brain with a tumour model (radius = 5 mm, $\varepsilon_r = 55$, $\sigma = 7$S/m) is simulated to acquire the E-field distribution.

Experiment 1) The CST 2011 Microwave Studio has a rich library of materials including some biomaterials such as bone, fat, and skin. Fig. 4 (a) shows the anatomical slice of the human head, which is basically composed of skin, fat, skull, grey matter and white matter. In our simulations, we used a human brain model, as shown in Fig. 4 (b). In this model, the main part is the white matter which has a radius of 60mm. Other parameters are as follows: bone thickness = 5mm, fat = 1mm, and skin = 1mm. A tumour with 5mm radius is placed in the white matter close to the skull.

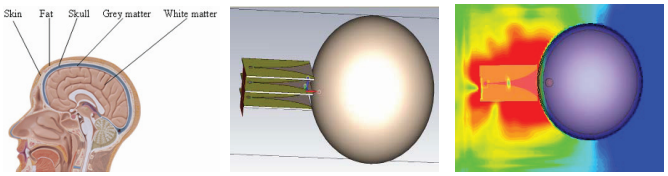

(a) (b) (c)

Fig. 4. (a) Anatomical slice of the human head, (b) the brain phantom and the vivaldi antenna array, (c) simulated E-Field distribution.

Fig. 4 (c) presents the top view of E-Field simulation results. It can be observed that the radiated signals penetrate the skin, fat, skull layers and finally reach the white matter. However, due to the backscatter from each layer, the energy attenuates very quickly. Therefore, only tumours close to the skull layer can be detected; otherwise, the reflected signal from the tumour could be too weak to be detected.

Experiment 2) Three vivaldi antennas are arranged to form an antenna array; one antenna as a transmitter and the other two as receivers. Here we use the notation O_{xy} to indicate the received signals, where y represents the transmitter and x the receiver antennas. Hence, O_{xy} refers to the signals which are transmitted by antenna y and received by antenna x. There are a total of 6 sets of received signals, which are O_{12}, O_{13}, O_{21}, O_{23}, O_{31} and O_{32}.

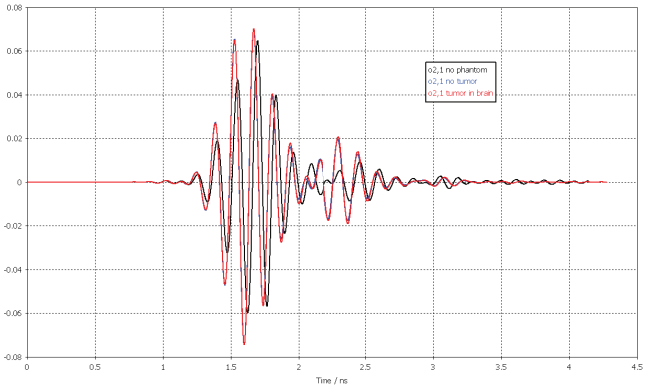

Fig. 5. Impulse responses received by antenna 2 from antenna 1.

Fig. 5 illustrates the impulse responses received by antenna 2 from antenna 1 (O_{21}) when the head phantom is not present (black line), antenna array faces the head phantom (red line, the tumour position is shown in Fig. 4 (c)) and without the tumour (blue line). It is observed that blue and red lines have a very similar profile; only the amplitude of the red line is slightly greater than the blue line. This is due to reflected signals by the tumour. As for the black line, it has the smallest amplitude and some time delay, especially for the time interval from 2ns to 2.5ns. This is due to no phantom presence to reflect signals. We can conclude that the time interval from 0 to 2ns represents the antenna array mutual coupling and multilayer reflection, whereas the remaining time interval shows the phantom response.

Simulation 1: Fig. 6 (a) and (b) are the top and side view of the simulation model, respectively. We insert one tumour model into the white matter model and change the tumour's location in the U-V Plane (Fig. 6 (a)), along the V axis (V= 0, -16, -32 and -45), while keeping the tumour steady in the W-U Plane (Fig. 6 (b)). The tumour locations P_3 (V= -32) and P_1 (V=0) are symmetric with respect to P_2 (V= -16). Normally, the antenna array is supposed to be rotated around the brain in order to obtain a set of different reflected signals from the tumour, which helps reduce noise. Instead, for convenience, we change the tumour's position which is equivalent to moving the antenna array around the brain.

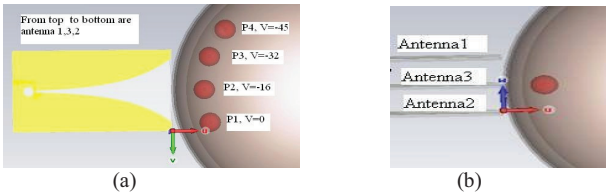

(a) (b)

Fig. 6. Schematic of the (a) U-V plane and (b) the W-U plane of the brain phantom model.

Fig. 7 (a) shows the signals received by the three receivers for the tumour located at V= 0, -16 -32 and -45. However, these curves are overlapped with each other. Therefore we select two sets of curves O_{21} (Fig. 7 (b)) and O_{31} (Fig. 7 (c)) for further analysis.

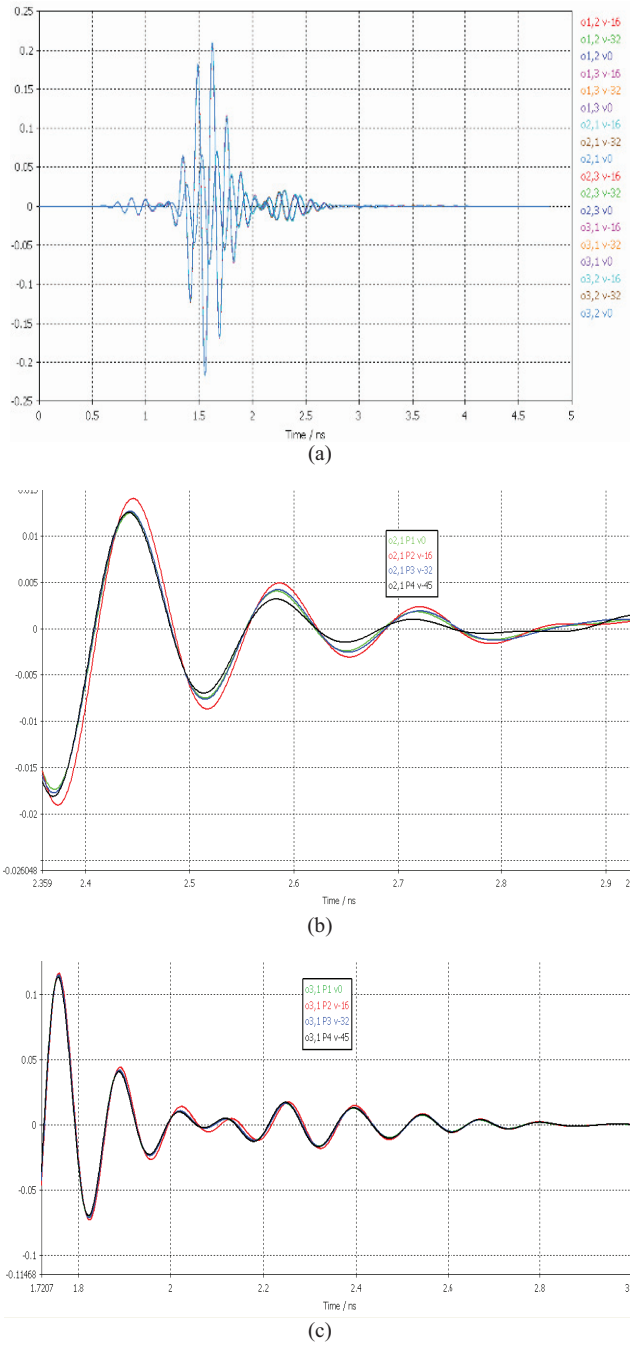

Fig. 7. Simulation results: (a) received signals, (b) antenna 2 and (c) antenna 3 received signals from antenna 1 when rotating the antenna array in U-V plane.

From Fig. 7 (b), it can be observed that there is a close match between green (V = 0) and blue curves (V = -32). This is due to their symmetric position, which leads to similar back scattered energy. However, both curves have lower amplitude in comparison with the red curve (V=-16). This is due to the location of the tumour. When the tumour is located at V= -16, it is right in the middle of the antenna array, so it reflects more energy. When the tumour is located at V= -45, it reflects less energy in comparison with the other three positions (P1, P2, P3), and hence it has the lowest amplitude. The received signal O_{31} (Fig. 7 (c)) has a similar profile to O_{21} since antenna 1 and antenna 3 are too close to each other, leading to a very strong mutual coupling, which immerses the backscattered signal from the tumour.

Simulation 2: In this case, the tumour changes position in the U-W Plane while it is kept steady in the U-V Plane. Fig. 8 (a) and (b) are the side and top view of the antenna array model. Fig. 9 shows the received signals O_{21} when the tumour is located at W= 0, 13.5, 27 and 40.5, respectively. It is observed that the amplitude difference of O_{21} is very small. This means that when changing the tumour location in the W-U Plane, the received signals from antenna 1 remain steady.

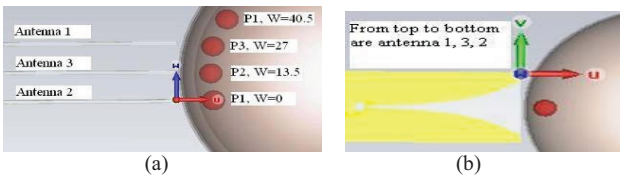

(a) (b)

Fig. 8. Schematic of the (a) U-W plane and (b) the U-V plane of the brain phantom model.

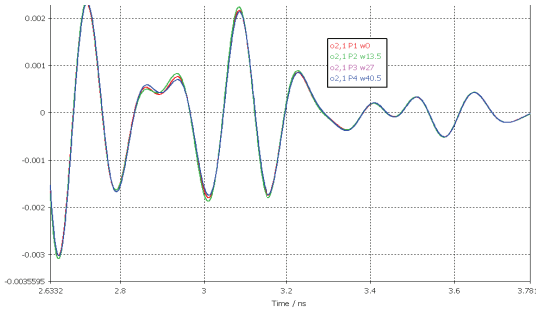

Fig. 9. Antenna 2 received signals from antenna 1 when rotating the antenna arrays in U-W plane.

IV. DISCUSSION AND CONCLUSIONS

Simulations 1 and 2 compare the different tumour locations. When the tumour moves in the U-V plane (Simulation 1, Fig. 6 (a)), the reflected signals have different amplitudes. On the other hand, the difference in amplitudes is very small when changing the tumour location in the U-W plane (Simulation 2, Fig. 8 (a)). From these simulations, it can be concluded that it is better to rotate the antenna array along the U-V plane.

Simulation 1 presents the received signal amplitudes when rotating the antenna array around the brain model. It shows that when the antenna array focuses on the tumour, received signals have the strongest amplitude. Otherwise, the amplitudes become weak when the focus point rotates away from the tumour. Fig.10 shows the received signal amplitudes for different tumour positions. When the antenna array

focuses to tumour at position P_2, the received signal has the strongest amplitude. The amplitude decreases when the antenna array's focus point moves to P_1, P_3, and P_4. Received signal amplitudes for the symmetric positions (P_1 and P_3) are close due to the uniform and slim radiation pattern of the vivaldi antenna arrays.

Impulse response from tumour can be observed from Fig. 7 (b), however, the antenna mutual coupling and multilayer reflection is still very strong. An approach to reduce the unwanted signal is to use impulse response from the phantom with tumour to subtract the impulse response without tumour [3]. Another method is to rotate the antenna array (simulation 1) and add the different impulse response curve coherently. The principle is when rotating the antenna array, a small change in distance between antenna array and phantom will lead to a great change for the impulse response of the tumour, however, the changes in the impulse response of the multilayer will not be that strong (can be observed in Fig. 7). So, when adding the different impulse response curves coherently, the tumour response part will be enhanced. Fig. 11 shows that after applying rotation calibration method, multilayer and tumour response part are slightly reduced and enhanced, respectively.

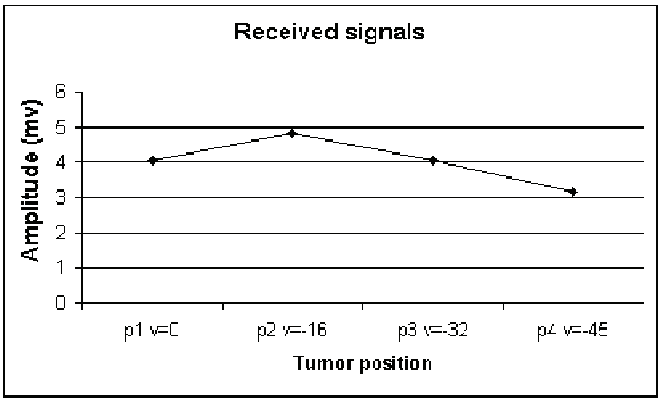

Fig. 10. The tumour position indicated by the received signals.

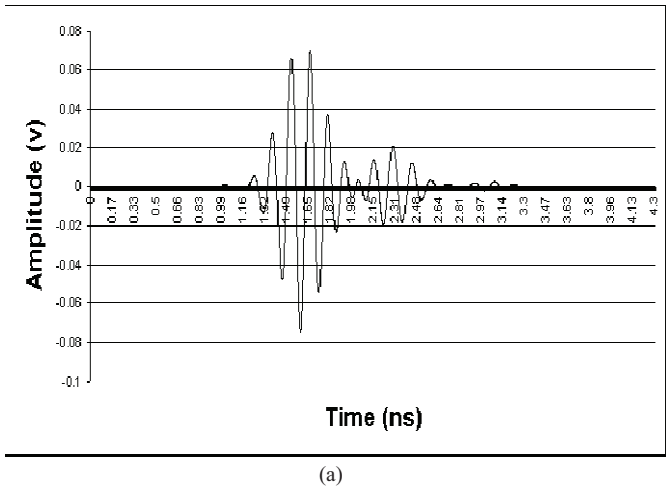

(a)

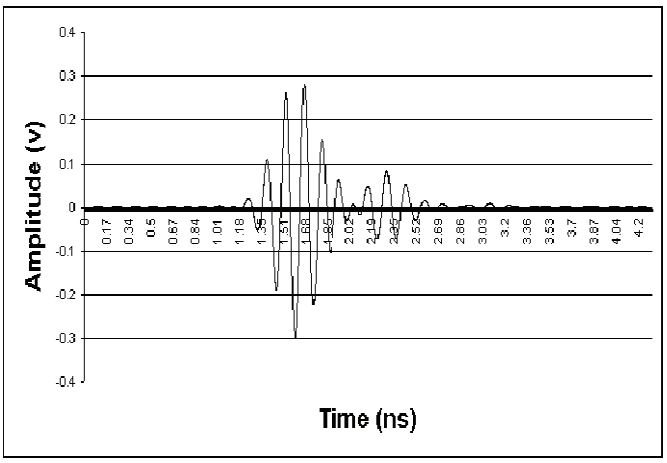

(b)

Fig. 11. Impulse response for (a) individual position (p4, from Fig. 8) and (b) rotation calibration method.

In this paper a smart antenna array based microwave imaging system for brain cancer detection has been presented. It was shown that when the antenna array focuses on the tumour, it scatters more energy in comparison with when the antenna array focus point moves away from the tumour. Using this knowledge, the tumour position can be determined by rotating the antenna array around the head. In addition, two approaches for rotating the antenna array around the head have been compared. The antenna array rotating in the U-V Plane illustrates a much better performance in comparison with rotating in the U-W Plane. From the simulation results, we can deduce that a UWB antenna based imaging system for brain cancer detection is feasible.

REFERENCE

[1] M.E. Bialkowski, Y. Wang, A. Abbosh, "UWB Microwave Monopulse Radar System for breast cancer detection," 2010 4th International Conference on Signal Processing and Communication Systems (ICSPCS), pp. 1-4, 13-15 Dec. 2010.

[2] Li, X.; Hagness, S.C.; Van Veen, B.D.; van der Weide, D. Experimental Investigation of Microwave Imaging via Space-Time Beamforming for Breast Cancer Detection; IMS: Philadelphia, PA, USA, June 8-13, 2003; pp. 379-382.

[3] S.C. Hagness, A. Taflove, and J.E. Bridges, "Two-dimensional FDTD analysis of a pulsed microwave confocal system for breast cancer detection: Fixed-focus and antenna-array sensors," IEEE Transactions on Biomedical Engineering, vol. 45, no. 12, pp. 1470–1479, Dec. 1998.

[4] F. Thiel, O. Kosch, F. Seifert, "Contrast agent based tumour detection by ultra-wideband radar: A model approach," 2010 Proceedings of the Fourth European Conference on Antennas and Propagation (EuCAP), pp.1-3, 12-16 April 2010.R. E. Sorace, V. S. Reinhardt, and S. A. Vaughn, "High-speed digital-to-RF converter," U.S. Patent 5 668 842, Sept. 16, 1997.

[5] D. Gibbins, M. Klemm, I.J. Craddock, J.A. Leendertz, I.J. Preece, R. Benjamin, "A Comparison of a Wide-Slot and a Stacked Patch Antenna for the Purpose of Breast Cancer Detection," IEEE Transactions on Antennas and Propagation, vol.58, no.3, pp.665-674, March 2010.

[6] E. Pancera, "Medical applications of the Ultra Wideband technology," 2010 Loughborough Antennas and Propagation Conference (LAPC), pp.52-56, 8-9 Nov. 2010.